Received: 4 April 2022 | Revised: 30 May 2022 | Accepted: 11 June 2022

DOI: 10.1049/rpg2.12532

IET Renewable Power Generation

The Institution of Engineering and Technology WILEY

ORIGINAL RESEARCH

Real option-based network investment assessment considering energy storage systems under long-term demand uncertainties

Shuang Cheng[1] | Chenghong Gu[1] | Ignacio Hernando-Gil[2] | Shuangqi Li[1] | Furong Li[1]

[1]University of Bath, Bath, UK

[2]ESTIA Institute of Technology, Bidart, France

Correspondence
Shuang Cheng, University of Bath, Bath, UK.
Email: sc2791@bath.ac.uk

Abstract

This paper proposes a novel real option (RO)-based network investment assessment method to quantify the flexibility value of battery energy storage systems (BESS) in distribution network planning (DNP). It applied geometric Brownian motion (GBM) to simulate the long-term load growth uncertainty. Compared with commonly used stochastic models (e.g. normal probability model) that assume a constant variance, it reflects the fact that from the point of prediction, uncertainty would increase as time elapses. Hence, it avoids the bias of traditional net present value (NPV) frameworks towards lumpy investments that cannot provide strategic flexibility relative to more flexible alternatives. It is for the first time to adopt the option pricing method to evaluate the flexibility value of distribution network planning strategies. To optimize the planning scheme, this paper compares the static NPVs and flexibility values of different investment strategies. A 33-bus system is used to verify the effectiveness of the formulated model. Results indicate that flexibility values of BESS are of utmost importance to DNP under demand growth uncertainties. It provides an analytical tool to quantify the flexibility of planning measures and evaluate the well-timed investment of BESS, thus supporting network operators to facilitate flexibility services and hedge risks from the negative impact of long-term uncertainty.

1 | INTRODUCTION

While numerous countries and regions have set ambitious carbon neutrality targets, the low-carbon development has led to a major energy paradigm shift. The increasing penetration of distributed energy resources (DERs), particularly those behind meters, leads to significantly volatile and unpredictable overall electricity demand [1]. For example, as reported by National Grid UK, the growing penetration of electric vehicles (EVs) could lift peak power demand by between 5 and 8 GWs by 2030. The situation is further aggravated by extensive electrification of heating and other sectors. These inevitable uncertainties pose high risks to distribution network planning. This may lead to a high likelihood of overinvestment because traditional network capacity reinforcement requires lump-sum investment. Conventional methods may cause a considerable portion of idle capacity and inefficient utilization of network infrastructure [2].

To hedge the risks in distribution network planning, alternative smart technologies can be adopted to enhance planning flexibility by deferring expensive traditional solutions until uncertainty unfolds over time [3].

Battery energy storage systems (BESS) can reduce system peak load and hence are essential to enable networks to integrate more renewable energy and volatile demand [4]. Thus, incorporating BESS into distribution network planning adds strategic opportunities for network reinforcement, which is an alternative to increase network investment flexibility and avert considerable overinvestment [5]. The investment flexibility discussed in this paper represents the capabilities of distribution network operators (DNOs) to defer investment in response to uncertainties.

Many researchers have studied the synergy between optimal BESS planning and distribution network upgrades. Technical and economic assessments are conducted to build optimization models for optimally sized and sited BESSs [6, 7]. The existing literature normally disregards the optimal investment time of BESS, leading to a bias towards lumpy investment strategies. Multi-stage investment is a widespread method to capitalize on the flexibility of strategic decision-making to address the risks of lumpy investment under long-term demand uncertainty. Diverse multi-stage models are proposed in the existing literatures. Paper [8] proposes a multi-stage expansion planning strategy for a district energy sector to optimize investment decisions. Paper [9] designs a multi-stage and stochastic planning model to integrate BESS and reactive power sources to increase the penetration of renewable generation. Papers [2] and [10] propose multi-stage distribution network planning methods to minimize the net present value (NPV) of the total investment and operational cost. However, the investment time intervals are fixed in these papers, that is, the optimal investment time is not considered in the planning. Because investment time is predetermined, whatever circumstances evolve, fixed multi-stage frameworks fail to unlock the flexibility of investment options fully.

In terms of flexibility assessment of BESS, some papers put an emphasis on optimization. For instance, paper [11] develops an optimal day-ahead scheduling model for multi-carrier BESS to assess its planning, operation, and flexibility contribution. Paper [5] investigates the energy storage allocation and investment optimization in terms of compressed air energy storage, pumped hydro storage, lithium-ion battery, and fly wheel. Nevertheless, most literature only addresses the flexibility valuation problem in the short run, for example, the energy scheduling stage. Limited efforts are devoted to quantifying the demand-side flexibility values from distribution network planning.

Compared to the existing investment assessment approaches, real option (RO)-based methods offer a well-founded framework to assess planning flexibility under long-term uncertainty [12]. Each planning scheme can be modelled as a portfolio of ROs that can be considered the right but not the obligation to perform investment [13]. Thus, their time values are incorporated into network planning. Some studies employ RO to solve transmission system planning problems. From the perspective of social planners, papers [14] and [15] present RO-based economic models for transmission expansion planning but do not specifically model power systems with detailed physical features.

In summary, there is very limited literature addressing distribution network investment (DNI) using RO. Although the paper [16] uses RO in distribution networks to quantify the flexibility value of demand response (DR) contracts, it only addresses the uncertainty of electricity prices to enable aggregators to hedge potential risks in the electricity market. However, volatile electricity prices are not the driving factor for distribution network reinforcement. Thus, the proposed model in [16] does not apply to distribution network planning. In the demand scenarios network innovation allowance (NIA) project [17], Electricity North West developed the RO-based assessment framework for DR under uncertainty in [18]. Although these models quantify the economic value of DERs against alternative investment strategies, they omit the physical electric network, the electric power flow and the corresponding operational constraints. Thus, it may lead to unreasonable economic assessment results, which inevitably limits its scalability for real-world distribution networks.

To address the research gap, this paper proposes an RO-based investment assessment model for BESS in distribution network planning (DNP), considering load growth uncertainties. Firstly, stochastic models are developed to model the uncertain behaviours of demand growth and renewable energy resources (RERs). After that, the expected incremental social welfares (ISWs) are estimated for BESS and traditional reinforcement methods through the investment revenue assessment model. This model evaluates the economic benefits from DNI portfolios when optimizing the operation of the whole distribution network. Thereafter, ISWs are input to the RO-based valuation model to quantify the flexibility values of available options embedded in DNP. The problem statements and proposed models are further illustrated as below.

1.1 | Problem statement

According to discount cash flow (DCF), upgrading projects are only carried out when the NPV of expected revenue can at least offset relevant costs. However, when assessing irreversible investment in power systems, the opportunity cost of investing an asset now rather than deferring it can be very high under even moderate uncertainties . Specifically, even though the static NPV of immediately investing BESS may not be big, it enables the option of lumpy and expensive investment to be alive until circumstances turn most favourable for exercising the option. By ignoring the value of deferral options, the cost-benefit analysis of multiple planning strategies only leads to now-or-never decisions that prevent investors from making or revising decisions in the future. As a result, since the conventional DCF planning framework uses static cash flows to assess planning solutions, it has a bias towards lumpy investment compared to more flexible alternatives that enable planners to react to unfolding information. Since 'deferral options' embedded in planning investment portfolios can offset the negative impact of uncertainties, it is essential to propose a novel method to quantify them fairly, which are added to DNI portfolios.

1.2 | Real option and investment assessment

Any attempt to assess the flexibility value (i.e. deferral option value) embedded in strategic DNI portfolios naturally leads to the concept of RO [3]. Borrowed from financial mathematics [19], an RO can be regarded as the option to defer and adjust investment decisions to solve uncertainty. Unlike traditional DCF, which assumes a passive management approach, RO seeks to value the flexibility embedded in an investment opportunity, for example, the flexibility of delaying the investment through time . The RO framework enables DNOs to make decisions on whether, how, and when BESS versus traditional network reinforcement assets should be implemented. Therefore, planners can seize these options to reduce the losses from overinvestment by adapting their future actions to respond to evolving future conditions.

The proposed methodology consists of stochastic modelling, an investment revenue assessment model and an RO-based flexibility valuation model. The assessment model quantifies cash flows originated by implementing DNI measures as an analogy for payoffs in economics. The result of the assessment model is input into the RO-based flexibility valuation model, which quantifies the value of available options embedded in different planning schemes, that is, corresponding flexibility value.

The main contributions of this paper are summarized below:

- This paper proposes a comprehensive method to evaluate the flexibility value of BESS in network planning, which can enable a more scalable analysis for DNOs from flexible investment. Unlike most planning models that use DCF to incorporate BESS in distribution network planning, this paper proposes an RO-based method to evaluate its flexibility value of BESS in network planning that can avoid the bias of traditional DCF frameworks towards lumpy investments relative to more flexible alternatives.
- Considering traditional fixed multi-stage investment strategies undervalue the flexibility in investment, this paper incorporates the option value into planning to investigate the impact of optimal investment time on DNI. The proposed valuation model takes the dynamic investment into account to hedge planning risks under long-term uncertainties, thus helping network operators to rationalize the design of flexibility contracts for BESS. Unlike the existing literature that assumes that investment is immediately performed or follows predetermined multi-stages, the proposed model can avoid the bias towards lumpy investments relative to more flexible alternatives.
- To better capture the stochasticity in demand growth, this paper employs a geometric Brownian motion (GBM)-based forecast model to represent the positive skewness of volatile load growth. Compared to commonly used stochastic models that assume constant variance, GBM can reflect that uncertainty would increase as time elapses from the point of prediction. Such a model has a lognormal probability density function to better capture the skewness of load growth uncertainty. Unlike fixed variance models, the proposed method adopts variable variances to reflect the fact that from the point of prediction, as time elapses, the accuracy of load forecast would decrease.

The remainder of this paper is organized as follows. Sections 2 and 3 illustrate the investment revenue assessment and RO-based flexibility valuation models. Section 4 presents the solution algorithm. Section 5 validates the performance of the proposed method through a modified IEEE 33-bus network. Section 6 summarizes the key findings in this paper.

2 | INVESTMENT REVENUE ASSESSMENT MODEL

Three parts are presented in this section: component-level modelling, network operation modelling, and incremental social welfare modelling. The network component modelling incorporates uncertain demand growth rates and renewable generation, that is, photovoltaics (PVs), and wind turbines (WTs). The network operation model optimizes the energy production cost. The operation cost reduction due to network investment is thus cumulated to assess the investment revenue through ISW. They are illustrated as below.

2.1 | Component-level modelling

2.1.1 | Stochastic modelling of peak demand growth rates

The uncertainty of load growth rate is modelled by developing the GBM model. The temporal change of load demand follows the underlying process:

$$dS(t) = \mu S(t) \times dt + \sigma S(t) \times dW(t) \tag{1}$$

$$dW(t) = \varepsilon(t)(dt)^{\frac{1}{2}} \tag{2}$$

$$E(S(t)) = \mathrm{S}(0) \times \mathrm{e}^{\mu t} \tag{3}$$

where $S(t)$ is the time-variant demand growth rate, $W(t)$ is the Wiener process, and $\varepsilon(t)$ is a serially uncorrelated and normally distributed random variable. Equation (1) denotes the mathematical expression of GBM. The former term models deterministic trends, while the latter models unpredictable events occurring during the time horizon. Equation (2) illustrates the continuous-time stochastic process, that is, the Wiener process. Equation (3) represents the corresponding expected value of load growth at time t. The stochastic model indicates that the current value of $S(0)$ is known to the planner, but the future growth rates are unknown, which follow lognormal distributions with a variance that grows linearly with time. Thus, the more distant the future positions, the more uncertain the circumstance is.

2.1.2 | RER modelling

This paper considers PVs, WTs, and BESS as DERs in distribution network planning. Solar output power [19] is shown as

$$P_{\mathrm{PV}} = \alpha \times A_s \times G_0 \times \int_0^1 f\left(G/G_0; \varphi_G; \sigma_G\right) \tag{4}$$

where G/G_0 scales G into [0,1]. The stochastic dynamics of PV production are modelled with φ_G andσ_G, which can be estimated through fitting Beta distribution into the mean and standard deviation of the observed solar irradiance. The solar output power is set as ±5% of the predicted value.

The extractable wind power [20] is shown as (5).

$$P_{WT} = \frac{1}{2} C_P \rho A V_{wt}^3 \tag{5}$$

2.2 | Operation modelling of distribution networks

2.2.1 | Objective function

The objective function of the distribution network operation is to minimize the total electricity supply cost, including the generation cost of thermal generating units and RER units, the power loss cost, and the load shedding cost, as shown in (6)–(11).

$$\min C = C_{WT} + C_{PV} + C_{TG} + C_{shed} + C_{grid} \tag{6}$$

$$C_{WT} = \sum_j p_{WT} \times P_{WT}^{i,j} \tag{7}$$

$$C_{PV} = \sum_j p_{PV} \times P_{PV}^{i,j} \tag{8}$$

$$C_{TG} = \sum_j \left(A\left(P_{TG}^{i,j}\right)^2 + BP_{TG}^{i,j} + C \right) \tag{9}$$

$$C_{shed} = \sum_b C_{LL,b}^i PL_{b,i} \tag{10}$$

$$C_{grid} = \sum_l p_{grid,i} \times P_{loss,l,i} \tag{11}$$

Equation (6) minimizes the energy supply cost of WTs, PVs, and traditional generators, the load shedding cost, and the grid loss cost. The energy supply costs can be calculated through (7)–(9), respectively. As shown in Equation (10), the load shedding cost C_{shed} is the cumulated product of the unsupplied load and value of lost load (VOLL). As shown in (11), the grid loss cost C_{grid} is derived through the real-time electricity price and the energy loss.

2.2.2 | Network operating constraints

The distribution network operation model is subject to the power flow constraints, the network capacity and security constraints, and the load shedding constraints, as clarified below.

$$PF_{b,c,i} = G_{b,c}\left(\sqrt{V_{b,i}} - \sqrt{V_{c,i}}\right) - B_{b,c}\left(\theta_{b,i} - \theta_{c,i}\right) + G_{b,c}\left(\frac{\left(\theta_{b,i} - \theta_{c,i}\right)^2}{2}\right) \tag{12}$$

$$QF_{b,c,i} = -B_{b,c}\left(\sqrt{V_{b,i}} - \sqrt{V_{c,i}}\right) - G_{b,c}\left(\theta_{b,i} - \theta_{c,i}\right) - B_{b,c}\left(\frac{\left(\theta_{b,i} - \theta_{c,i}\right)^2}{2}\right) \tag{13}$$

$$\underline{V} \leq V_{b,i} \leq \bar{V} \tag{14}$$

$$\underline{P_{PV}} \leq P_{PV} \leq \overline{P_{PV}} \tag{15}$$

$$\underline{P_{WT}} \leq P_{WT} \leq \overline{P_{WT}} \tag{16}$$

$$\underline{P_{TG}} \leq P_{TG} \leq \overline{P_{TG}} \tag{17}$$

$$0 \leq PL_{b,i} \leq PD_{b,i} \tag{18}$$

Constraints (12) and (13) enforce the active and reactive power balance based on the new optimal power flow (OPF) model in [21]. Since the traditional OPF model cannot address power losses, the linear OPF model provides a more accurate calculation. Constraint (14) enforces the nodal voltage security. Constraints (15)–(17) ensure the electricity generation volumes of WT, PV, and traditional generators are within their capacity. Constraint (18) ensures that the unsupplied load does not exceed the actual demand at each bus [22].

2.2.3 | BESS constraints

The operation constraints of BESS are illustrated as below

$$Q^i = Q_{sc}^i + Q_{sd}^i \tag{19}$$

$$Q_{sc}^i \leq 0 \tag{20}$$

$$Q_{sd}^i \geq 0. \tag{21}$$

$$E_-^i \geq S_{min}^i \tag{22}$$

$$E_+^i \leq S_{max}^i. \tag{23}$$

$$E_{\lambda}^{i} = -\lambda \left(\eta_{\text{in}} PB_{i}^{C} + \frac{1}{\eta_{\text{out}}} PB_{i}^{D} \right) \tag{24}$$

$$E_{-}^{i} \le E_{-}^{i-1} + E_{\lambda}^{i} - \lambda \frac{\eta_{\text{loss}}}{2} \left(E_{-}^{i} + E_{-}^{i-1} \right) \tag{25}$$

$$E_{+}^{i} \ge E_{+}^{i-1} + E_{\lambda}^{i} - \lambda \frac{\eta_{\text{loss}}}{2} \left(E_{+}^{i} + E_{+}^{i-1} \right). \tag{26}$$

$$\sum_{s \in \Phi_{\text{SB}}} PB_{b,s,i}^{C} + PD_{b,i} + \sum_{c} PF_{b,c,i} = \sum_{j \in \Phi_{\text{GB}}} \left(\sum_{j} P_{\text{WT}}^{i,j} + \sum_{j} P_{\text{PV}}^{i,j} + \sum_{j} P_{\text{TG}}^{i,j} \right) + \sum_{s \in \Phi_{\text{SB}}} PB_{s,i}^{D} + PL_{b,i} \tag{27}$$

$$\sum_{s \in \Phi_{\text{SB}}} QB_{\text{s},i}^{C} + QD_{b,i} + \sum_{c} QF_{b,c,i} = \sum_{j \in \Phi_{\text{GB}}} \left(\sum_{j} Q_{\text{WT}}^{i,j} + \sum_{j} Q_{\text{PV}}^{i,j} + \sum_{j} Q_{\text{TG}}^{i,j} \right) + \sum_{s \in \Phi_{\text{SB}}} QB_{\text{s},i}^{D} + QL_{b,i}. \tag{28}$$

$$E_{s,b,i=1} = E_{s}^{0} \tag{29}$$

$$E_{s,b,i} = E_{s}^{0} + \sum_{i=1}^{i-1} \eta_{\text{in}} \times PB_{s,b,i}^{C} - \sum_{i=1}^{i-1} \frac{PB_{s,b,i}^{D}}{\eta_{\text{out}}} \tag{30}$$

$$0 \le E_{s,b,i} \le Y_{b} E_{s}^{\text{rated}}, s \in \Phi_{\text{SB}} \tag{31}$$

$$\sum_{i=1}^{i} \eta_{\text{in}} \times PB_{s,i}^{C} = \sum_{i=1}^{i} \frac{PB_{\text{s},i}^{D}}{\eta_{\text{out}}} \tag{32}$$

Constraint (19) demonstrates that the net energy injection Q^{i} for BESS is the sum of charging and discharging power injections at time i. Constraints (20) and (21) ensure the charging and discharging limits. Constraints (22) and (23) enforce BESS's energy lower and upper bounds. Constraints (24)–(26) implement the charging and discharging constraints during the scheduling time for BESS. Constraints (27) and (28) ensure the active and reactive power balance, respectively. BESS acts as loads in charging mode and as generators at discharging mode. Thus, the charging power of BESS contributes to the total electricity generation, while the discharging power contributes to the energy consumption. In such a case, BESS can mitigate network congestion by: (1) increasing energy consumption when there is low demand or high penetration; (2) providing additional generation capacity when there is high demand or low generation. Constraints (29) represent that at the beginning of daily scheduling, E_{s}^{0} is stored in BESS at time $i = 1$. As shown in (30), the stored energy in the subsequent time slots is a function of the initial constant stored energy E_{s}^{0}, the charging and discharging power, and the corresponding efficiencies. Constraint (31) limits the capacity of candidate BESS. Constraint (32) ensures operational consistency, that is, the initial value of the stored energy equals that at the end of each scheduling period.

2.3 | Incremental social welfare

To assess the payoffs of different investment options, this part cumulates the operation cost savings on time horizon T to represent the incremental social welfare. It can evaluate the present value of economic profits from exercising planning measures in year t. The detailed model formulation is clarified as follows:

$$\Pi \left(n, \omega, t_{\text{n}}, X_{t_n} \right) = PV(ISW)_{\gamma,\omega,t_n} - I_{\text{total},\omega,t_n} \tag{33}$$

$$PV(ISW)_{\gamma,\omega,t} = \sum_{y=t}^{T} \frac{ISW_{\gamma,\omega}(y)}{(1+r)^{y}} \tag{34}$$

$$ISW_{\gamma,\omega}(y) = \sum_{i=1}^{8760} \left(C_{y,\text{i},\omega,\text{base}}^{\text{total}} - C_{y,\text{i},\omega,\text{inv}}^{\text{total}} \right) \tag{35}$$

$$I_{\text{total},\omega,t_n} = \sum_{s \in \Phi_{SB}} \frac{Y_s I_{s,\omega,t_n}}{(1+\rho)^{t_n}} + \sum_{l \in \Phi_{CL}} Z_l I_{l,\omega,t_n} \tag{36}$$

$$C_{j,i,\omega}^{\text{total}} = C_{\text{sup},j,i,\omega} + C_{\text{shed},j,i,\omega} + C_{\text{gird},j,i,\omega} + CC_{j,i,\omega}. \tag{37}$$

$$CC_{j,i,\omega} = \sum_{l=1}^{\Phi_l} \left(pf_{j,i,l} - C_l \right) \times U_{\text{c}} \tag{38}$$

Constraint (33) defines the payoff function $\Pi(n, \omega, t_n, X_{t_n})$ which is calculated by subtracting the investment cost from the present value of ISW. As defined in (34) and (35), ISW is the cumulated operation cost savings throughout each investment stage, which is discounted to the present value through the discount rate r. It should be noted that both the traditional network investment and BESS can mitigate network congestion and thus reduce operation costs, yet with different approaches. Traditional wire solutions can increase the branch capacity C_l, while BESS can reduce peak power flows $pf_{j,i,l}$. Equation (36) represents that the total investment cost consists of BESS and feeder expansion costs. The BESS investment capital cost drops with a decay rate ρ. The operation and investment assessment models are coordinated through Equations (37), representing that the total operation cost consists of the energy supply, load shedding, power loss, and network congestion cost. The network congestion cost is formulated in (38) based on the C/D method proposed in [23].

3 | RO-BASED FLEXIBILITY VALUATION MODEL

The objective function of flexible distribution network planning is to maximize the expectation of the discounted payoff function $\Pi(n, \omega, t_n)$ so that optimal investment decision-making can be achieved. In other words, the planning scheme is optimized when the expected net profits from the well-timed investments are maximized in terms of BESS and capacity. It is formulated as

$$F\ (n,\omega,t_n) = \max\ E\left[\Pi\,(n,\omega,t_n)\right], s\ \times\ t\ \times\ t_n \in (0,T) \tag{39}$$

where $E[\cdot]$ denotes the expectation operator. Since it is expected to obtain the total maximized payoffs with uncertain decision-making in each investment stage, the problem reduces to seeking the optimal investment time throughout the planning horizon along each sample path. To solve the problem, this paper refers to Bellman's principle of optimality, that is, the optimal decision-making policy has the basic principle that regardless of the initial state and decisions, the remaining decisions must constitute an optimal policy in terms of the state resulting from the first decision. Thus, the objective function can be expressed as below

$$F\ (n,\omega,t_n) = max\left\{\Pi\,(n,\omega,t_n)\,, E^*_{t_n}\left(F\left(n+1,\omega,t_{n+1}\right)\right)\right\}. \tag{40}$$

$$\phi^*\ \left(\omega,t_n,X_{t_n}\right) = E^*_{t_n}\ \left(F\left(n+1,\omega,t_{n+1}\right)\right) \tag{41}$$

where $F(n,\omega,t_n)$ represents the flexibility value of all investment options available at time t_n, while $E^*_{t_n}(F(n,\omega,t_{n+1})$ is defined as the continuation value, that is, the estimated payoff from continuation rather than exercising the investment option at time t_n. Equation (40) demonstrates that the optional stopping policy (i.e. the optimal investment time for each planning measure) is determined by comparing the economic value of an immediate investment, that is, $\Pi(n,\omega,t_n)$ and the value of deferring the investment to the future, that is, $E^*_{t_n}(F(n,\omega,t_{n+1})$. Equation (41) uses $\phi^*(\omega,t_n,X_{t_n})$ to demonstrate the continuation value of available investment options at time t_n. Since the investment time of available options at t_n is uncertain, the continuation value is unknown to the system operator. This paper uses the least square method (LSM) algorithm to estimate the continuation value. The ways of estimating the continuation value and obtaining the optimal investment time are formulated in (42)–(46).

$$E^*_{t_n}(F\ \left(n+1,\omega,t_{n+1}\right) = \underset{\partial}{min} \sum_{!\,=\,1}^{\Omega}\left[\Pi\left(n+1,\omega,t_{n+1},\ X_{t_{n+1}}\right)(1+r)^{-1} - \sum_{p\,=\,1}^{P}\partial_p \times L_p\left(X_{t_n}\right)\right]^2 \tag{42}$$

$$L_p\left(X_{t_n}\right)\ =\ \exp\left(-\frac{X_{t_n}}{2}\right)\frac{e^{X_{t_n}}}{p!}\frac{d^p}{dX_{t_n}^p}\left(X_{t_n}^p e^{-X_{t_n}}\right) \tag{43}$$

$$\phi^*\ \left(\omega,t_n,X_{t_n}\right) = \sum_{p=1}^{P}\partial^*_p\cdot L_p\left(X_{t_n}\right). \tag{44}$$

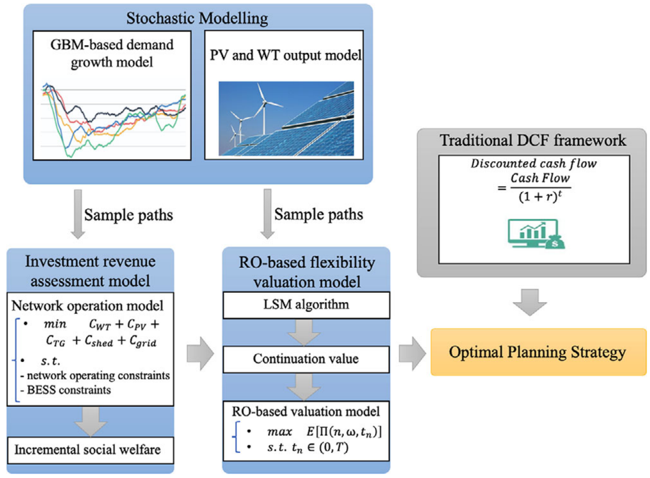

FIGURE 1 Framework of the proposed methodology

$$\phi^*\ \left(\omega,t_n,X_{t_n}\right) \le \Pi\left(n,\omega,t_n,\ X_{t_n}\right) \tag{45}$$

$$F\ \left(X_{\tau(\omega)}\right) = \frac{1}{\Omega}\sum_{!\,=\,1}^{\Omega}\Pi\left(n,\omega,\tau\left(\omega\right),X_{\tau(\omega)}\ \right)\ \times (1+r)^{-\tau(\omega)}. \tag{46}$$

where L_p ($p = 1, 2, \ldots, P$) is the orthonormal basis of the state variable X_{t_n}. Equation (42) estimates the continuation value $E^*_{t_n}(F(n+1,\omega,t_{n+1})$ by regressing from the discounted future payoffs, that is, $\Pi(n+1,\omega,t_{n+1},\ X_{t_{n+1}})(1+r)^{-1}$ on a linear combination. Equation (43) represents the orthonormal basis of the used linear function of the state variable X_{t_n}. The optimal coefficient ∂^*_p can be obtained by solving the optimization problem (42) and (43). After that, the estimated continuation value can be derived through (44). Working backwards from $t_n = T$ to $t_0 = 0$, the optimal investment time can be obtained by comparing the value from the continuation and the 'payoff' from immediate exercising. As illustrated in (45), the investment option will be exercised only when the current payoff is larger than the continuation value. The comparison criteria are performed for all sample paths calculated from the uncertainty model throughout the investment horizon. The loop works backwards from the end of the planning stage and does not end until $n = 0$. At the maturity of investment options, the continuation value is zero. Equation (46) calculates the option value, that is, the flexibility value based on the optimal investment time $\tau(\omega)$ for sample path ω. As shown in (46), the flexibility value is obtained by discounting and cumulating the payoffs throughout the time horizon.

The stochastic models for RER and load growth, investment revenue assessment, and flexibility valuation models are coordinated to achieve the optimal DNP, as shown in Figure 1. The stochastic model produces sample paths based on Monte Carlo. For each sample path, the investment revenue assessment model and the RO-based flexibility valuation mode are sequentially performed to calculate the flexibility values of different planning schemes. The former model assesses cash flows

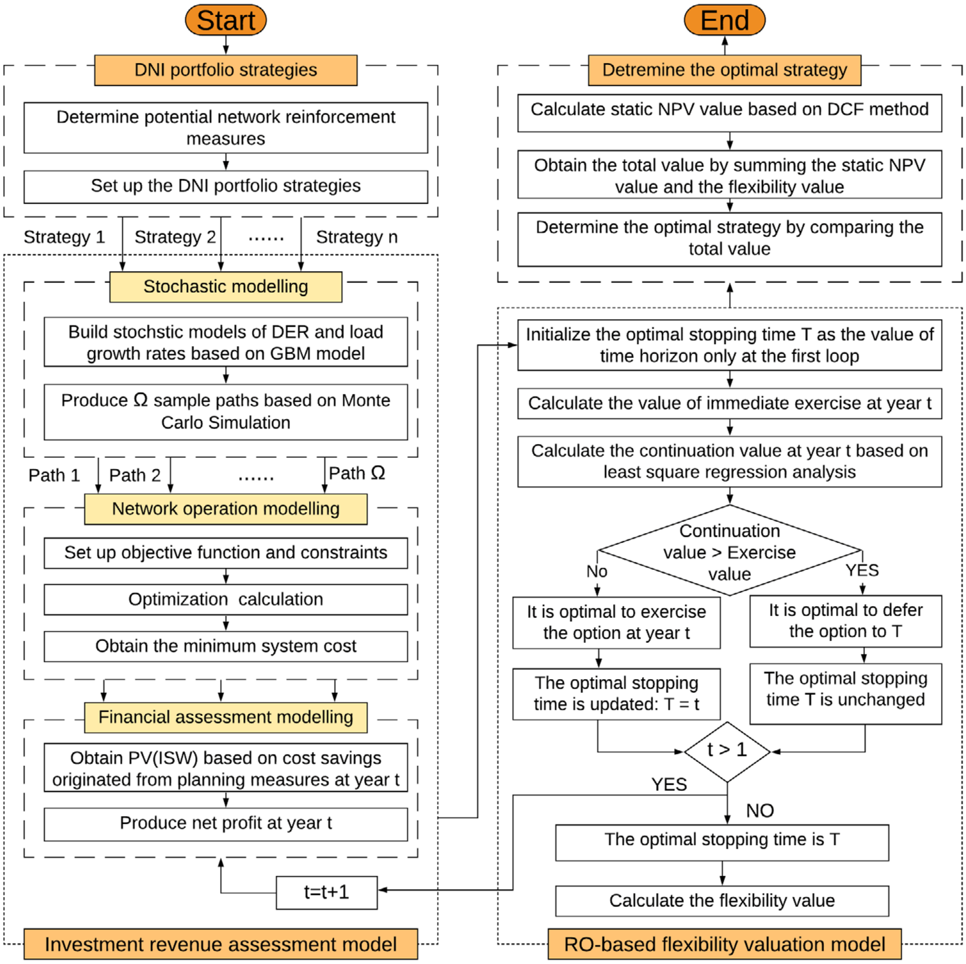

FIGURE 2 Solution algorithm of the proposed methodology

originated by implementing investment measures and input to the latter model. The latter model quantifies the total value of available investment options embedded in different planning schemes. The static NPVs of planning strategies are calculated from the traditional DCF framework. Finally, by adding and maximizing the flexibility value and the static NPV value, the proposed method acquires the optimal planning strategy for the distribution network.

4 | IMPLEMENTATION

The RO-based flexibility valuation model is solved by an algorithm developed from dynamic programming, as shown in Figure 2. The proposed LSM-based implementation algorithm is originated from the least-squares approach. This paper uses it here because: (i) it is an approach that is intuitive, accurate, easy, and computationally efficient to evaluate American-style options. Its efficiency has been verified by using a number of realistic examples; (ii) considering the time horizon is unlikely to be very large, the proposed implementation algorithm is fast enough to find the optimal stopping time in network planning.

The procedures for implementing the proposed method are summarized as follows:

1. Firstly, the stochastic modelling of DER and load growth rates is performed to produce sample paths, where the GBM model and Monte Carlo simulation are applied.
2. The RO-based flexibility valuation model is conducted to obtain the optimal stopping rule (e.g. the optimal investment time of different planning measures through all paths) and the corresponding flexibility values. Specifically, by comparing the exercise value that is calculated through network operation modelling and the continuation value that is obtained through LSM, the optimal stopping time is found, working backwards from the last year to the first year.
3. The network operation modelling is embedded in the valuation model, where the load data, the network constraints, and the siting data of BESS are updated if the sample path or the time index changes. The operation results are output to the valuation model to compute the payoff function.

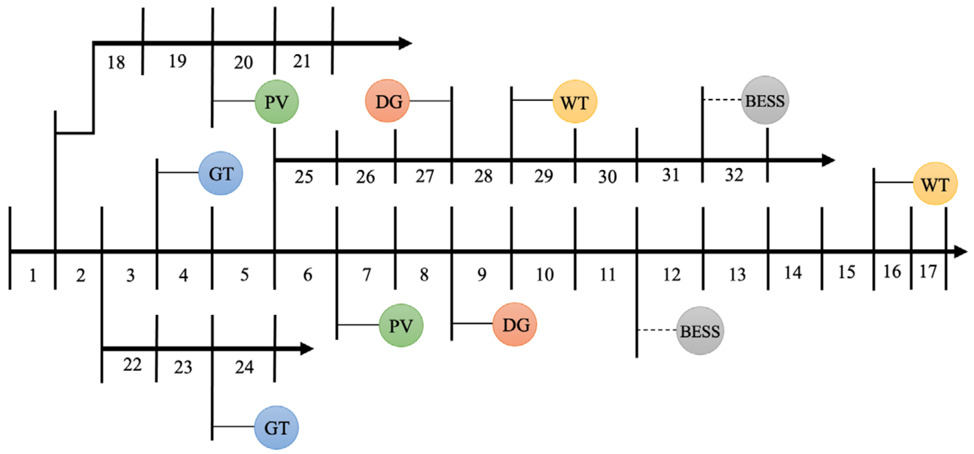

FIGURE 3 IEEE 33-bus system

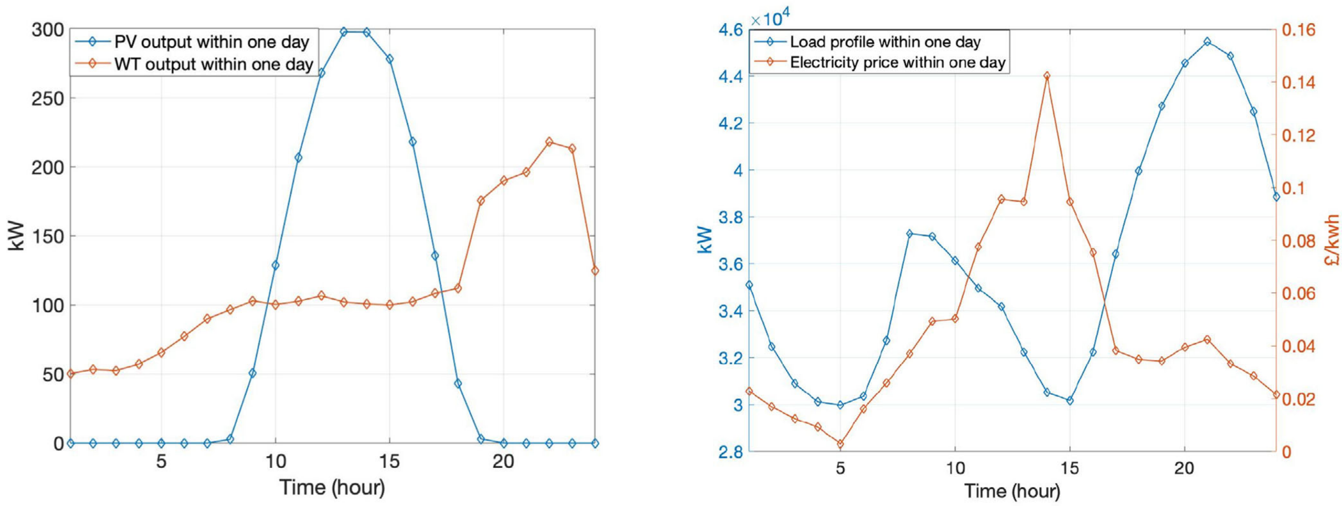

(a) Daily PV and WT production curves (b) Daily electricity price and load profile

FIGURE 4 Daily PV and WT production curves. PV, photovoltaics; WT, wind turbines.

4. The total values for the planning schemes are calculated by adding the flexibility value that is obtained from the valuation model and the static NPV that is calculated by the DCF method.

5 | CASE STUDY

To assess the performance of the proposed methodology, a modified IEEE 33-bus test system is used as a case study, as shown in Figure 3. This network has eight generating units, that is, two WTs, two PVs, two diesel generators, and two gas-fuelled generators [24]. Branch 1 is the most congested network component and needs reinforcement. The daily PV and WT production curves are illustrated in Figure 4a, while the daily electricity price and load profiles are shown in Figure 4b.

TABLE 1 Economic parameters

Parameter	Value
Feeder cost coefficient (£/MVA)	100,000
Energy cost coefficient for BESS (£/kWh)	500
Weighted average cost of capital (WACC)	6.9%

The original capacity of all distribution lines is set as 5 MVA. The economic data are demonstrated as shown in Table 1. Table 2 illustrates the technical parameters of DERs and BESS. The parameters of the GBM model are shown in Table 3. The drift and volatility values are determined by referring to the National Grid's annual Future Energy Scenarios Report [25].

Traditionally, expanding the capacity of branch 1 is a capital-intensive but effective planning strategy with stable load growth.

TABLE 2 Parameters of BESSs and DERs

Parameter	Value
Maximum power of the micro gas turbine (kW)	300
Minimum power of the micro gas turbine (kW)	100
Maximum power of the diesel generator (kW)	250
Minimum power of the diesel generator (kW)	100
Maximum charging power of BESS (kW)	−200
Maximum discharging power of BESS (kW)	250
Capacity of invested BESS (kWh)	200
Capacity of the expanded feeder (MVA)	10
The discount factor for BESS capital costs (%)	15

TABLE 3 Parameters of the stochastic model

Parameter	Value
Simulated paths based on GBM	2000
Initial load growth rate (%)	1
Exercise points per year	5
The percentage drift μ (%)	3
The percentage volatility σ (%)	51
The correlation coefficient	0.44

However, considering the uncertainty of electricity demand growth, it introduces high risks for DNOs. In comparison, investing in BESS can postpone the irreversible investment of new lines until up-to-date information indicates the investment is inevitable. Thus, it provides flexible and economical solutions for DNP. In this case study, expanding branch 1 and investing in BESS are assumed two investment options available in the first year. The planning strategies are thus categorized into four cases:

1. S1: Investing in BESS in the first year;
2. S2: Expanding branch 1 in the first year;
3. S3: Investing in branch 1 and BESS in the first year;
4. S4: Taking no network expansion planning measures in the first year until further information is obtained.

Given that S3 possesses no available investment options through the time horizon, there is no further managerial flexibility embedded in it. Specifically, the flexibility value of S3 is zero.

5.1 | Results

Assuming that the planning time horizon is 25 years, the stochastic behaviour of the load growth rate is simulated on the time horizon with 2000 paths, as shown in Figure 5. The red line in Figure 6 represents the expected value of growth rates at time t, as shown in (3). The black, blue, yellow, and green lines

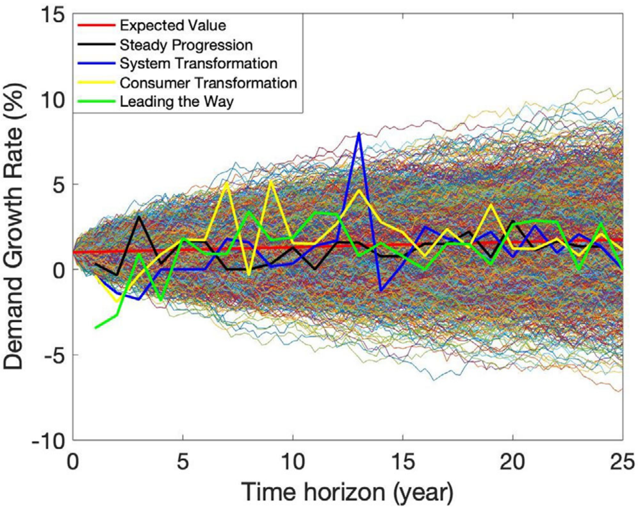

FIGURE 5 Random behaviour of the demand growth based on the GBM model. GBM, geometric Brownian motion

simulate peak demand growth predicted by National Grid in its annual Future Energy Scenarios Report [21]. They represent the demand growth in four future scenarios, for example, steady progression, system transformation, consumer transformation, and leading the way, respectively. As shown in the figure, the parameters ensure that the average demand simulated growth rate trajectory (e.g., the red line) is aligned with the four future scenario trajectories.

Meanwhile, the 2000 simulated trajectories are sufficiently dispersed around their average to present a broad range of predicted future scenarios. The stochastic dynamics of demand fluctuations appropriately reflect the relationship between load growth uncertainty and time. Specifically, the load growth rate can be predicted with a small deviation in the distant future, for example, varying from 0% to 2% in the first year. Nevertheless, there exists a high diversity of demand growth rates in the last few years during the time horizon, for example, varying from −2% to 14% in the last year.

Based on the investment revenue assessment model, the present values of estimated annual economic benefits and cumulated net profits from three investment strategies over the time horizon are diagrammed, as shown in Figures 6, 7, and 8. They play significant roles in quantifying the flexibility values of different investment strategies under long-term uncertainty. These figures indicate the potential payoffs and flexibility values of different strategies (i.e., investment in BESSs or branch 1 first) under different future scenarios at different future time points. It can demonstrate that deferring the traditional expensive investment in the first year has higher flexibility values based on the assumptions in this paper. Considering the focus of this paper is flexibility evaluation, we think they are essential in the result analysis. They also illustrate that with time elapse, the flexibility values of available investment options decrease, until 0 in the final year over the planning horizon.

Taking Figure 6 as an example, there are three axes, that is, time, path, and values. The 'time' illustrates the future time

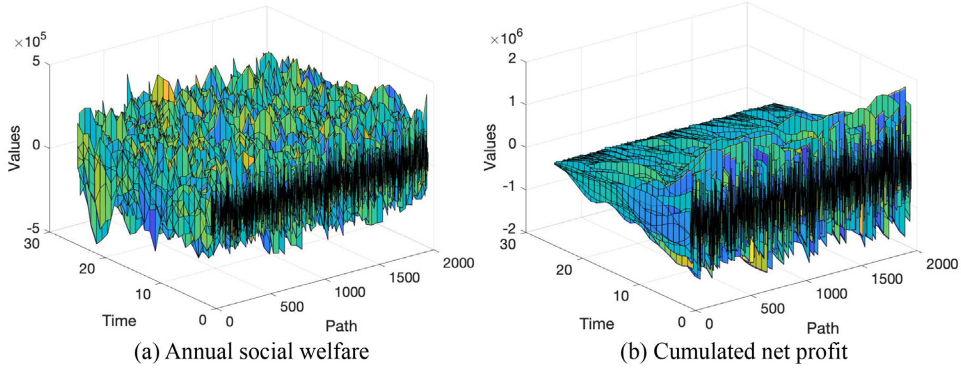

FIGURE 6 Annual social welfare and cumulated net profit of Strategy 1

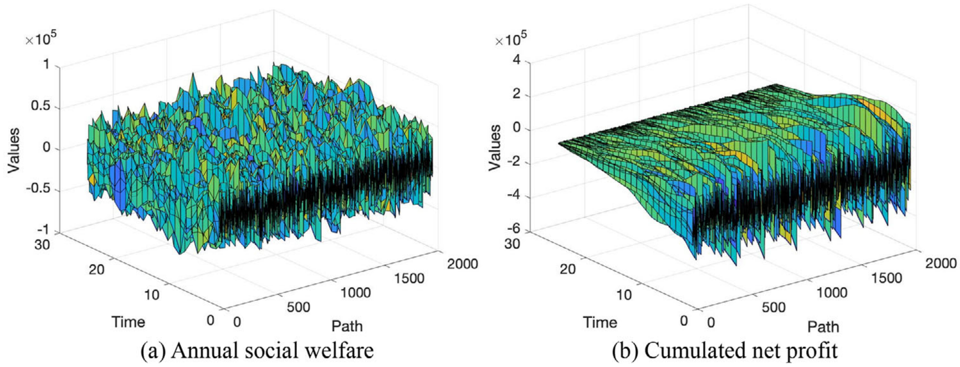

FIGURE 7 Annual social welfare and cumulated net profit of Strategy 2

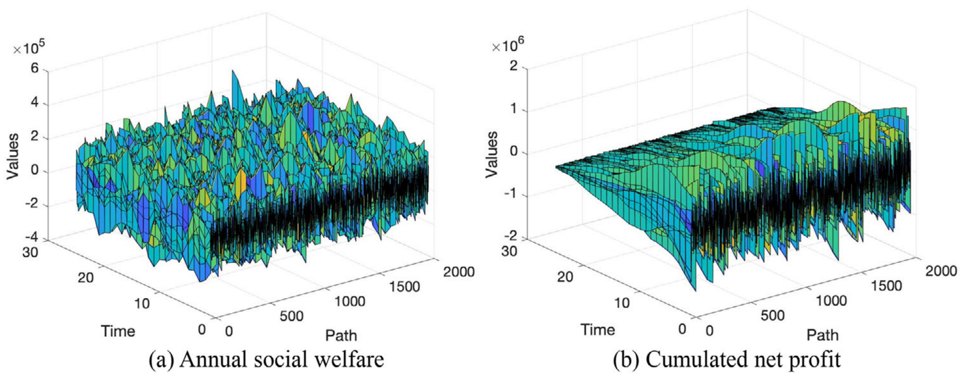

FIGURE 8 Annual social welfare and cumulated net profit of Strategy 4

over the planning horizon (i.e. 25 years). The 'path' denotes the sample paths, that is, the simulated future scenarios in terms of peak demand growth. The 'values' means the annual social welfare (i.e. the cost reduction) and the cumulated net profit of strategy 1 (i.e. deploying BESSs in the first year). Figure 6a shows the various payoffs of deferring the expensive investment in branch 1 in different time points and different future demand growth scenarios over 25 years. Figure 6b shows the cumulated values of deferring the traditional investment, that is, the flexibility values of available investment options under different predicted demand growth scenarios and investment time points. As shown in the figure, the annual cost reductions of the available option vary from around £-5×10^5 to £3×10^5 during the time horizon, while the cumulated net profit varies from £-1.8×10^6 to £1.8×10^6. That means keeping the investment option of feeder expansion alive could lead to cost reductions from around £-5×10^5 to £3×10^5 and option values from £-1.8×10^6 to £1.8×10^6. As shown in Figure 7, the annual cost reductions of deferring investment of BESSs vary from £-5×10^4 to £7×10^4, while the option values differ from £-4×10^5 to £2×10^5. Since there are no flexibility values for S3, the proposed model is not applied to it. For S4, no measures

TABLE 4 Economic parameters ranking of strategies based on the proposed valuation approach and the traditional DCF method

Strategy	Expected project value ($\times 10^4$£)	Static NPV ($\times 10^4$£)	Flexibility value ($\times 10^4$£)
S1	20.797	1.810	18.987
S2	9.022	8.010	1.012
S3	9.816	9.816	0
S4	19.932	0	19.932

are taken initially, thus keeping both options available. Figure 8 presents that the potential cost reductions of both investment options vary from £-3×10^5 to £3.5×10^5, while the option values vary from £-2×10^6 to £1.5×10^6. In conclusion, keeping both investment options alive has the highest peak option value and the lowest valley value.

There are 2000 sample paths at each investment time interval during the planning horizon, for example, 25 years. The annual social welfare represents the total cost reductions from exercising available options in a particular year. The cumulated net profit (e.g. the payoff function Π) represents the cumulated value of available options, which is the difference of incremental ISW and reinforcement costs from a particular year to the end of the time horizon. In other words, it denotes the option value from keeping options open and enabling them to be exercised in a particular year.

The RO-based flexibility valuation model is implemented by initially identifying the continuation value through the LSM algorithm. Therefore, the optimal stopping rules are generated for the three planning strategies, which are statistically illustrated in Figure 9. Each path has an optimal investment time (i.e. optimal stopping time) of the available option for these three strategies. Figure 9 aggregates the number of sample paths with the same optimal stopping time range. The optimal stopping time of 25 indicates that the available options will not be exercised during the planning horizon. It can be found in Figure 9a that under the given circumstances, there is a high likelihood of exercising the available options in the first few years or not exercising them during the whole time horizon for S1. For S2, the years when the option will be exercised are more decentralized. In comparison, even though S4 holds two available expansion options, they are likely to be exercised during the first few years due to the inevitable requirements for network reinforcement.

Table 4 presents the static NPVs, the flexibility values, and the total expected values for the four planning strategies. The static NPVs are calculated from the traditional DCF method, while the flexibility values are derived from the proposed model. It can be found that Strategies S1 and S4 have considerable flexibility values. The economic importance of keeping the investment option of BESS open and deferring it to the future is around 18.987$\times10^4$£. Keeping both investment opportunities alive in the first year is estimated as 19.932 $\times10^4$£. According to the traditional method, S3 is the optimal planning scheme, that is, investing in branch 1 and BESS in the first year. However, since S3 stops DNO from revising the original investment decision-

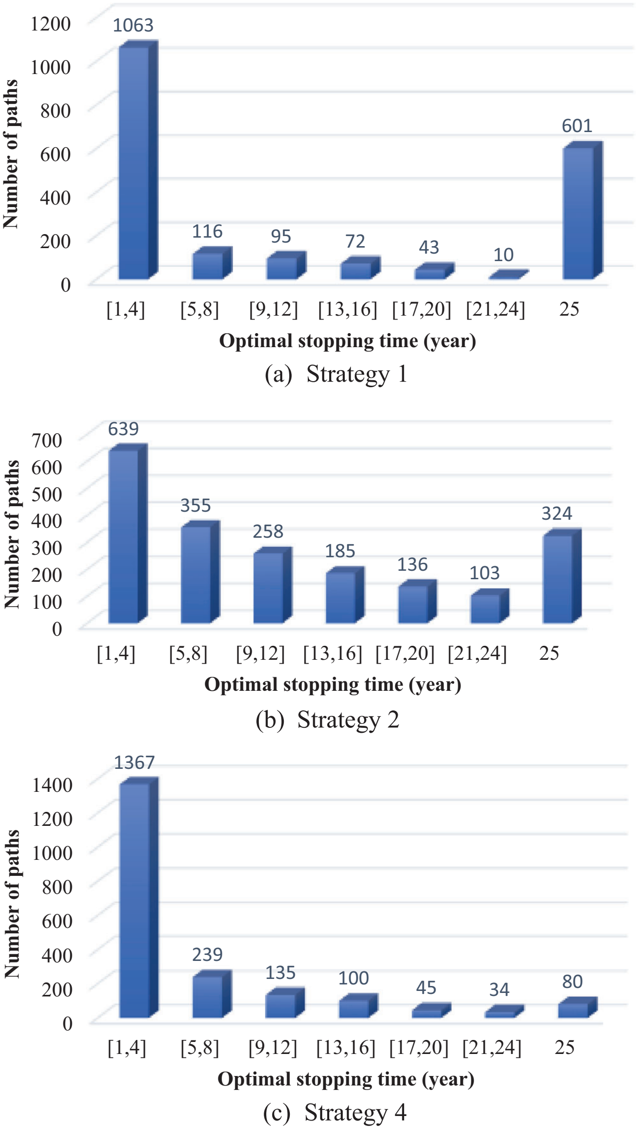

FIGURE 9 Stopping rules for multiple network reinforcement plans

making in the future, it has no flexibility values. The results from the proposed method suggest that S1 is the optimal planning scheme under demand uncertainty.

5.2 | Discussion

The discussion part presents the sensitivity analysis for key variables and the performance of the computation simplification method.

5.2.1 | Sensitivity analysis

The sensitivity analysis shows how the flexibility value varies with stochastic parameters and the time horizons. Firstly, a sensitivity analysis is performed with different values of the percentage volatility in the stochastic model, as shown in Table 5.

TABLE 5 Flexibility value and the total value of three strategies with variable values of the percentage volatility

Volatility	Flexibility value($\times 10^4$£)			Total value ($\times 10^4$£)		
	S1	S2	S4	S1	S2	S4
0.1	17.53	1.28	16.82	19.34	9.29	16.82
0.2	18.29	1.29	18.03	20.10	9.30	18.03
0.3	18.70	1.30	18.53	20.51	9.31	18.53
0.4	18.99	1.35	19.93	20.80	9.36	19.93
0.5	19.29	1.36	22.69	21.10	9.37	22.69
0.6	19.46	1.38	24.65	21.27	9.39	24.65
0.7	20.48	1.49	27.00	22.29	9.50	27.00

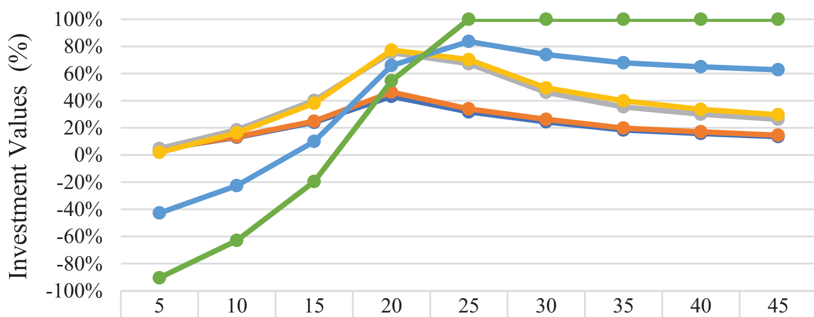

	5	10	15	20	25	30	35	40	45
Static NPV (×10^4£) S3	-41.76	-28.92	-17	-4.28	9.82	20.54	36.61	49.95	65.34
Static NPV (×10^4£) S2	-39.09	-27.82	-16.17	-4.31	8.01	19.32	32.02	44.83	58.05
Static NPV (×10^4£) S1	-2.51	-1.56	-1.21	0.75	1.81	2.61	5.05	5.08	5.83
Flexibility value (×10^4£) S4	0.59	3.65	8.81	10.97	19.93	15.65	17.79	18.45	20.61
Flexibility value (×10^4£) S2	0.04	0.29	0.48	1.19	1.35	1.45	1.62	1.77	1.82
Flexibility value (×10^4£) S1	3.54	9.3	13.82	16.34	18.99	19.25	21	22.57	23.72

Time Horizon (year)

Flexibility value (×10^4£) S1
Flexibility value (×10^4£) S2
Flexibility value (×10^4£) S4
Static NPV (×10^4£) S1
Static NPV (×10^4£) S2
Static NPV (×10^4£) S3

FIGURE 10 Flexibility values and NPVs of four planning strategies with variable time horizons

The percentage volatility makes no difference to the static NPV, which ignores the uncertainty of load growth, that is, £1.81 × 10^4, £8.01 × 10^4, £9.816 × 10^4, and 0 with the volatility of 0.4 for the four strategies, respectively. Additionally, since S3 holds no available options, its flexibility value remains zero. Therefore, Table 5 only presents the flexibility values and total values of the three strategies, given that higher volatility values imply larger uncertainty. Table 5 shows that flexibility values rise with the volatility since the available options are more valuable under higher uncertainty. Remarkably, S1 is always the optimal strategy until the volatility value is higher than 0.4. Hence, where the market is uncertain, there is a strong incentive to wait and keep the investment options alive rather than exercise them. Under such circumstances, network reinforcement measures should be deferred until uncertainty gets resolved over time.

Figures 10 and 11 show the effect of the planning time horizon on the results. It can be found that both the flexibility value and the static NPV value are sensitive to the time horizon. Specifically, all three numerical results grow accordingly with the incremental time horizon. With a shorter planning time horizon, the profit horizon shrinks while the capital costs are constant. In addition, since the uncertainty grows significantly with increasing time horizons, the flexibility value is more sensitive than the static NPV value. Thus, there is also a positive correlation between the total value and the time horizon. In addition, the total value of Strategy S2 outstrips S1 when the time horizon is 35 years, indicating that investing feeders is more valuable than the storage system with a longer time horizon.

5.2.2 | Computation simplification

This paper uses the test results with the same model parameters to evaluate the effectivity of the approximation method,

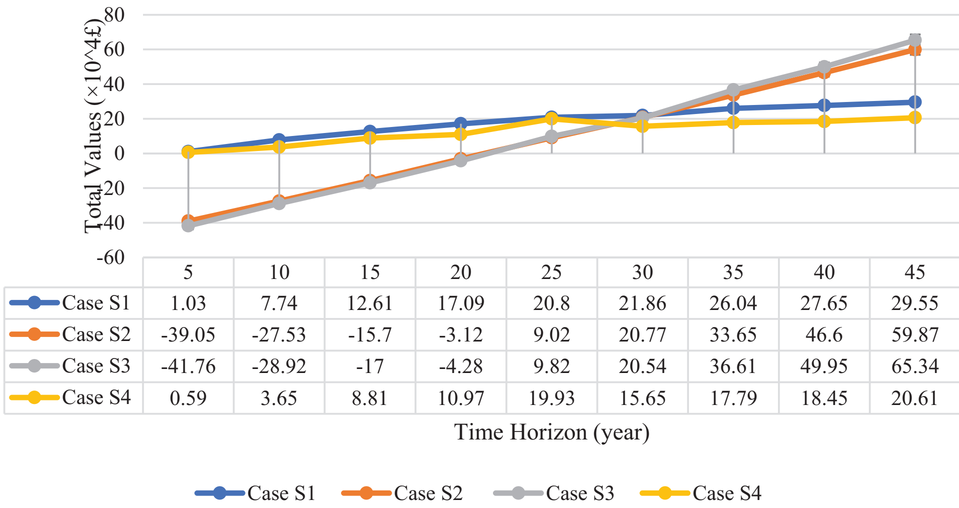

	5	10	15	20	25	30	35	40	45
Case S1	1.03	7.74	12.61	17.09	20.8	21.86	26.04	27.65	29.55
Case S2	-39.05	-27.53	-15.7	-3.12	9.02	20.77	33.65	46.6	59.87
Case S3	-41.76	-28.92	-17	-4.28	9.82	20.54	36.61	49.95	65.34
Case S4	0.59	3.65	8.81	10.97	19.93	15.65	17.79	18.45	20.61

FIGURE 11 Total investment values of four planning strategies with variable time horizons

TABLE 6 Diagnostic test results

Planning strategy	Actual value ($\times10^4$£)	Approximation value ($\times10^4$£)	Time without approximation (s)	Time with approximation (s)	Deviation rate (%)
S1	18.987	18.751	22807.829	5673.428	1.24
S2	1.349	1.362	20900.047	5721.316	0.96
S4	19.932	19.531	22315.102	5655.156	2.01

as shown in Table 6. The elaborate simulation process calculates the option value without approximation. By comparison, the value with an approximation is calculated by using the regression function parameters in the sample to estimate the continuation values out of the sample. As shown in the table, the differences in flexibility values between the two methods are negligible, while the execution time reductions are remarkable. Thus, the simplification approach is recommended to minimize the computational time.

6 | CONCLUSION

This paper develops an RO-based model to explore the managerial flexibility and time value of DNI schemes. The extensive case study indicates that the traditional DCF analysis leads to sub-optimal solutions when it is used to evaluate planning projects involving managerial flexibility under long-term uncertainty. Additionally, the flexibility value of planning measures is sensitive to stochastic parameters of load growth. The proposed approach offers analytical tools for simultaneously assessing the flexibility values of planning strategies and determining the optimal solution. Through the proposed method, a trade-off between the revenues of investment in large traditional feeders and the flexibility of investment in BESS is achieved.

FUNDING INFORMATION

The author(s) received no specific funding for this work.

CONFLICT OF INTEREST

None.

DATA AVAILABILITY STATEMENT

The data that support the findings of this study are available from the corresponding author upon reasonable request.

NOMENCLATURE

Indices and sets

b, c	Index for network node in set Φ_B
i	Index for scheduling time
j	Index for generation units in set Φ_{GB}
l	Index for network branch
n	Index for time interval in set N
N	Set of discrete intervals
s	Index for BESS unit in set Φ_{SB}
t, y	Index for exercise year
γ,ω	Index for planning measure and sample path
Ω	Set of sample paths from Monte Carlo
Φ_B, Φ_{GB}	Set of network nodes and generation units

Φ_{SB}	Set of candidate BESSs
Φ_{EL}, Φ_{CL}	Set of the existing line and candidate line

Abbreviations

WT	Wind Turbines
DER	Distributed Energy Resources
EV	Electric Vehicles
DNO	Distribution Network Operators
V2G	Vehicle-to-Grid
DNP	Distribution Network Planning
BESS	Battery energy storage systems
GBM	Geometric Brownian Motion
RO	Real Options
DNI	Distribution Network Investment
NPV	Net Present Value

Parameters

A_s	Array surface area in square meters
ρ, A	Air density and area swept by blades
α	Solar panel efficiency
G_0, G	Extra-terrestrial and global horizontal radiation
μ	Vector drift of GBM
σ	Percentage volatility of GBM
φ_G, σ_G	Simulation parameters of stochastic PV production
λ	Scheduling time length for BESS
η_{in}, η_{out}	BESS Charging and discharging efficiency
η_{loss}	Hourly energy loss of BESS
r	The weighted average cost of capital
ρ	Annual discount rate for BESS investment
τ	Stopping time, i.e., investment time

Variables

A	Cost factors for traditional generators
C_l	Capacity of network branch l
C_{WT}, C_{PV}, C_{TG}	The operation costs of WT, PV, and traditional generators, respectivelyc
C_{shed}	Cost of unsupplied load
$C_{base}^{total}, C_{inv}^{total}$	Total cost of the base case and the investment case
$C_{sup}, C_{shed}, C_{grid}, CC_{j,i,\omega}$	Energy supply, load shedding, imported power, and congestion cost, respectively
$C_{LL,b}^{i}$	Value of Lost Load (VOLL)
E	Energy injected into or stored from the system from BESS
E_s^{rated}	Rated capacity of BESS s
E_-^i, E_+^i	Energy lower and upper bounds on the energy stored in BESS at time i
$G_{b,c}, B_{b,c}$	Line conductance and susceptance between buses b and c
I	Investment cost
p_{WT}, p_{PV}	Unit price of WT and PV, respectively
$p_{grid,i}$	Real-time electricity wholesale price
$pf_{j,i,l}$	Power flow on congested branch l
$\underline{P}, \bar{P}$	Power limits of generators
P_{grid}	Imported power from the wholesale market
$P_{WT}^{i,j}, P_{PV}^{i,j}, P_{TG}^{i,j}$	Power output of wind turbine, PV, and traditional generators, respectively
PB^C, PB^D	Active charging and discharging power
PD, QD	Active and reactive power demand
PF, QF	Active and reactive power flow between buses b and c
PL, QL	Active and reactive unsupplied power
Q_{sc}^i, Q_{sd}^i	Charging and discharging power injections at time i, respectively
QB^C, QB^D	Reactive charging and discharging power
$Q_{WT}^{i,j}, Q_{PV}^{i,j}, Q_{TG}^{i,j}$	The reactive power output of WTs, PVs, and traditional generators
S	Peak demand growth rate
S_{min}^i, S_{max}^i	Minimum and maximum stored energy limits for BESS at time i
T	Planning horizon
U_c	Unit congestion cost
V, θ	Voltage magnitude and angle
$\underline{V}, \bar{V}$	Voltage security lower and upper limits
V_{wind}	Area swept by blades
dW	Weiner process
Y, Z	Binary variable for the investment state of BESS and feeder
X	State variable
τ	Optimal stopping time
$\varepsilon(t)$	Serially uncorrelated and normally distributed random variable

ORCID

Shuang Cheng https://orcid.org/0000-0002-1002-4407

REFERENCES

1. Adebayo, T.S., Rjoub, H., Akinsola, G.D., Oladipupo, S.D.: The asymmetric effects of renewable energy consumption and trade openness on carbon emissions in Sweden: new evidence from quantile-on-quantile regression approach. Environ. Sci. Pollut. Res. 29(2), 1875–1886 (2022)
2. Koutsoukis, N.C., Georgilakis, P.S.: A multistage distribution network planning method considering distributed generation active management and demand response. IET Renewable Power Gener. 16(1), 65–76 (2022)
3. Cheng, S., Gu, C., Yang, X., Li, S., Fang, L., Li, F.: Network Pricing for Multienergy Systems Under Long-Term Load Growth Uncertainty. IEEE Trans. Smart Grid 13(4), 2715–2729 (2022)
4. Ghatak, S.R, Sannigrahi, S., Acharjee, P.: Optimised planning of distribution network with photovoltaic system, battery storage, and DSTATCOM. IET Renewable Power Gener. 12(15), 1823–1832 (2018)
5. Yacar, D., Tejada-Arango, D.A., Wogrin, S.: Storage allocation and investment optimisation for transmission-constrained networks considering losses and high renewable penetration. IET Renewable Power Gener. 12(16), 1949–1956 (2018)
6. Li, S., Gu, C., Xu, M., Li, J., Zhao, P., Cheng, S.: Optimal power system design and energy management for more electric aircrafts. J. Power Sources 512, 230473 (2021)
7. Li, S., Zhao, P., Gu, C., Huo, D., Zeng, X., Pei, X., Cheng, S., Li, J.: Online battery-protective vehicle to grid behavior management. Energy 243, 123083 (2022)
8. Yang, W., Liu, W., Chung, C.Y., Wen, F.: Coordinated Planning Strategy for Integrated Energy Systems in a District Energy Sector. IEEE Trans. Sustainable Energy 11(3), 1807–1819 (2020)

9. Ding, T., Hu, Y., Bie, Z.: Multi-stage stochastic programming with nonanticipativity constraints for expansion of combined power and natural gas systems. IEEE Trans. Power Syst. 33(1), 317–328 (2018)
10. Gangwar, P., Singh, S.N., Chakrabarti, S.: Multi-objective planning model for multi-phase distribution system under uncertainty considering reconfiguration. IET Renewable Power Gener. 13(12), 2070–2083 (2019)
11. Keihan Asl, D., Hamedi, A., Reza Seifi, A.: Planning, operation and flexibility contribution of multi-carrier energy storage systems in integrated energy systems. IET Renewable Power Gener. 14(3), 408–416 (2020)
12. Cheng, S., Gu, C., Yang, X., Li, J.: Real options based optimal planning for integrated energy systems under long-term uncertainties. pp. 1–5.
13. Cheng, S., Gu, C., Zhang, Y., Li, J., Li, F.: Real Options based Investment Decision Making for Distribution Networks under Long-term Uncertainties. pp. 1–5.
14. Mariscal, F., Reyes, T., Sauma, E.: Valuing flexibility in transmission expansion planning from the perspective of a social planner: A methodology and an application to the Chilean power system. The Engineering Economist 65(4), 288–320 (2020)
15. Henao, A., Sauma, E., Reyes, T., Gonzalez, A.: What is the value of the option to defer an investment in Transmission Expansion Planning? An estimation using Real Options. Energy Economics 65, 194–207 (2017)
16. Schachter, J.A., Mancarella, P.: Demand response contracts as real options: a probabilistic evaluation framework under short-term and long-term uncertainties. IEEE Trans. Smart Grid 7(2), 868–878 (2015)
17. Shaw, R.: Distribution Network Planning:A 'Real Options' approach to support decisions on reinforcement versus post-fault demand-side-response (DSR). In Energy Management: Flexibility, Risk and Optimisation, Edinburgh (2016)
18. Schachter, J.A., Mancarella, P., Moriarty, J., Shaw, R.: Flexible investment under uncertainty in smart distribution networks with demand side response: Assessment framework and practical implementation. Energy Policy 97, 439–449 (2016)
19. Yan, X., Gu, C., Li, F., Wang, Z.: LMP-based pricing for energy storage in local market to facilitate PV penetration. IEEE Trans. Power Syst. 33(3), 3373–3382 (2018)
20. Yang, Y., Mok, K., Tan, S., Hui, S.Y.: Nonlinear dynamic power tracking of low-power wind energy conversion system. IEEE Trans. Power Electron. 30(9), 5223–5236 (2015)
21. Yuan, H., Li, F., Wei, Y., Zhu, J.: Novel linearized power flow and linearized OPF models for active distribution networks with application in distribution LMP. IEEE Trans. Smart Grid 9(1), 438–448 (2018)
22. Mehrjerdi, H., Hemmati, R.: Modeling and optimal scheduling of battery energy storage systems in electric power distribution networks. J. Cleaner Prod. 234, 810–821 (2019)
23. Yan, X., Gu, C., Li, F., Wang, Z.: LMP-based Pricing for Energy Storage in Local Market to Facilitate PV Penetration. IEEE Trans. Power Syst., 1-1 (2017)
24. Zimmerman, R.D., Murillo-Sánchez, C.E.: MATPOWER user's manual, Power Systems Engineering Research Center (PSerc) (2019)
25. *National Grid's Annual Future Energy Scenarios Report*, National Grid ESO (2020)

How to cite this article: Cheng, S., Gu, C., Hernando-Gil, I., Li, S., Li, F.: Real option-based network investment assessment considering energy storage systems under long-term demand uncertainties. IET Renew. Power Gener. 16, 2778–2792 (2022). https://doi.org/10.1049/rpg2.12532